

Evaluation of Separation Mechanism Design for the Orion/Ares Launch Vehicle

Kevin E. Konno*, Daniel A. Catalano*, Thomas M. Krivanek*

Abstract

As a part of the preliminary design work being performed for the Orion vehicle, the Orion to Spacecraft Adaptor (SA) separation mechanism was analyzed and sized, with findings presented here. Sizing is based on worst case abort condition as a result of an anomaly driving the launch vehicle engine thrust vector control hard-over causing a severe vehicle pitch over. This worst case scenario occurs just before Upper Stage Main Engine Cut-Off (MECO) when the vehicle is the lightest and the damping effect due to propellant slosh has been reduced to a minimum. To address this scenario and others, two modeling approaches were invoked. The first approach was a detailed Simulink model to quickly assess the Service Module Engine nozzle to SA clearance for a given separation mechanism. The second approach involved the generation of an Automatic Dynamic Analysis of Mechanical Systems (ADAMS) model to assess secondary effects due to mass centers of gravity that were slightly off the vehicle centerline. It also captured any interference between the Solar Arrays and the Spacecraft Adapter. A comparison of modeling results and accuracy are discussed. Most notably, incorporating a larger SA flange diameter allowed for a natural separation of the Orion and its engine nozzle even at relatively large pitch rates minimizing the kickoff force. Advantages and disadvantages of the Simulink model vs. a full geometric ADAMS model are discussed as well.

Introduction

A component of the Vision for Space Exploration, Orion will be capable of carrying crew and cargo to the ISS, or rendezvous with a lunar landing module and an Earth departure stage in low-Earth orbit to carry crews to the moon and, one day to Mars-bound vehicles assembled in low-Earth orbit. Orion borrows its shape from the capsules of the past, but it takes advantage of 21st century technology in computers, electronics, life-support, propulsion and heat protection systems. Orion will be launched into low-Earth orbit by the Ares I Crew Launch Vehicle. To maximize the crew's safety, Orion and its abort system will be placed at the top of the Ares I rocket. Other means of abort are available after the Launch Abort System is jettisoned at ~75 km (250,000 ft). The Orion vehicle will be able to remain docked to ISS for up to six months and have the ability to stay in lunar orbit untended for the duration of a lunar surface visit that could be up to six months.

A separation mechanism design is being developed to assure clearance between Orion (Crew Exploration Vehicle and Service Module) and the Spacecraft Adapter (SA) which stays fixed to the Ares upper stage as the two vehicle elements separate from each other during both normal post-launch staging or in an abort event. Figure 1 depicts the Ares/Orion stack configuration prior to separation.

The preliminary design of the separation mechanism requires the balancing of several competing design parameters most notably sufficient kickoff forces to ensure separation, highly reliable components, limited space to house these mechanisms, and a requirement to keep the mechanisms lightweight due to tight mass budgets. The abort case will typically drive the size of the separation mechanism design for a crewed vehicle. Activation of the separation mechanism cannot occur until the thrust levels of the Ares I Upper Stage (US) are significantly reduced. The potential hard-over gimbal abort case can induce a severe pitch over rate (often referred to as "dump rate") of up to 35 degrees/second on the stack if it were to occur just before Upper Stage Main Engine Cut-Off (MECO) when the vehicle is the lightest and the damping effect due to propellant slosh has been reduced to a minimum. The transients of the controls

*NASA Glenn Research Center, 21000 Brookpark Road Cleveland, OH 44135

and engine thrust tail-off (~ 3 sec total from hard-over to low thrust) are the main reason a large dump rate can be induced. A Residual Engine Thrust (RET) also continues to induce a small force at 5 degrees off the vehicle centerline resulting in an applied moment to the Upper Stage after separation. This defines the worst case environment that the separation mechanisms must overcome. Recontact during either an abort separation, or a nominal separation, can be catastrophic resulting in a Loss of Mission (LOM) or a Loss of Crew (LOC) event. A recent example of this type of detrimental recontact was observed during the March 2007 SpaceX Corporation Falcon I launch first stage separation event in which the first stage adapter inner wall contacted the second stage engine nozzle and induced a propellant slosh in the second stage tanks, prematurely shutting down the second stage engine before reaching the proper orbit [1]. The Orion separation system must be adequately sized to reliably separate the crew and vehicle safely for all design cases. Multiple types of mechanisms were evaluated including spring actuators, constant pressure pneumatic actuators, and pyrotechnic-actuated gas thrusters.

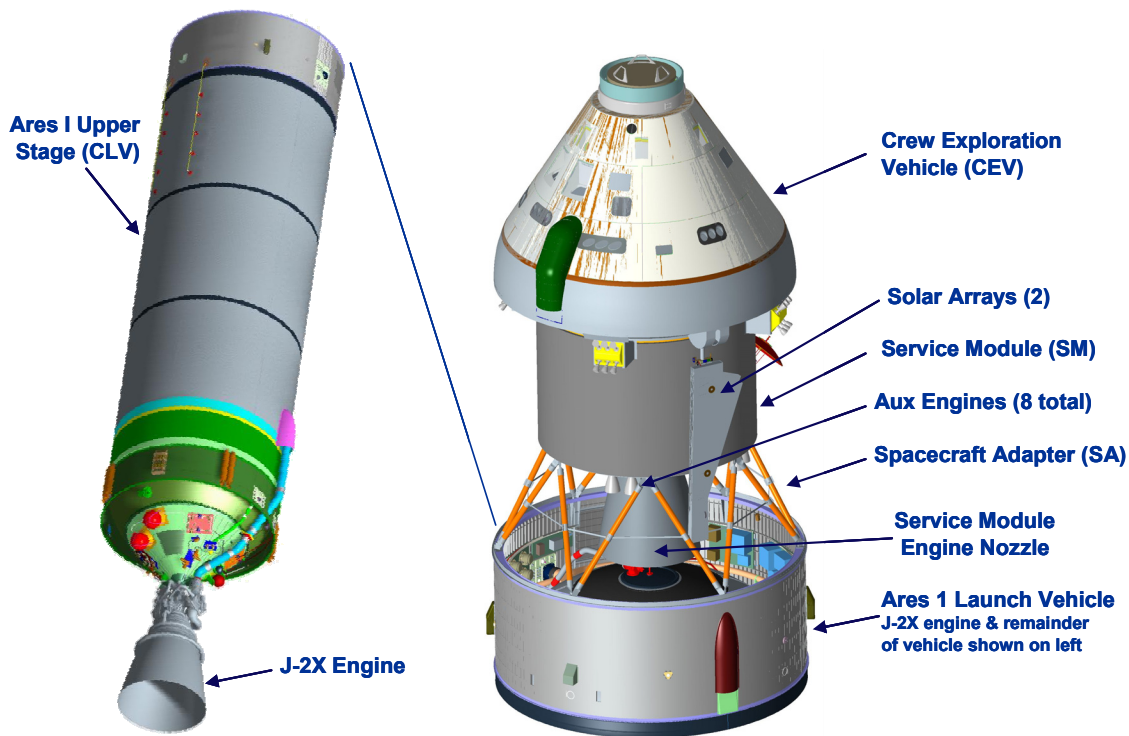


Figure 1. Ares I Upper Stage/Orion Spacecraft Configuration (Lockheed Martin Concept)

The Point of Departure (POD) separation system is shown in Figure 2. Unlike Apollo's Service Module which was bolted to the top of a four piece faring and severed from it via a circumferential linear shape charge, this system incorporates compression kickoff springs and pyrotechnic separation bolts to join the Orion Vehicle to the SA. Separation is triggered by firing the pyrotechnic retention bolts, which allows the compression springs to push the SM away from the Upper Stage. The spring force must be sufficient to accelerate the separated bodies away from each other while maintaining a minimum clearance throughout separation.

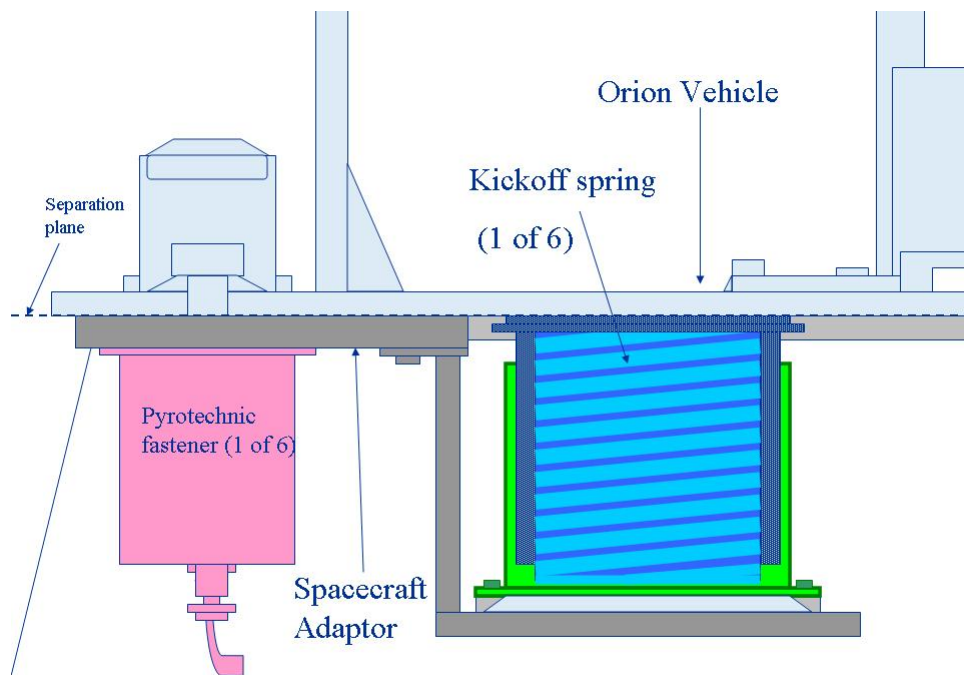


Figure 2. Separation Spring Concept

Separation System Hardware

The force needed for separation can be generated from various competed technologies, including mechanical springs, pneumatic actuators or gas thrusters. The other components of interest in the staging mechanism are the pyrotechnic fasteners through which the launch loads are transmitted.

Mechanical Springs: For this study open coiled, helical, compression springs were the preferred form of kickoff devices if the required energy level was low enough to warrant their use. Spring kickoff devices were incorporated in most of the models because the separation environment did not require large kickoff forces. Obviously, mechanical springs are used in countless terrestrial applications as well as space. They are highly reliable and when designed correctly can handle millions of cycles. Several papers detail the use of compression springs in spacecraft staging mechanisms [2], [3], [4], [5], [6], [7], [8]. For spacecraft mechanisms mechanical kickoff springs must be designed with the resistive force (F_r) and the force required for acceleration (F_a) of the bodies in mind. Where redundant springs are used instead of a backup mechanism they should be designed to provide adequate force for a one-spring-out case [5].

Additionally, the spring system should have a 100% positive Margin of Safety (MS) on drive force over resistive force, as measured at acceptance or qualification testing. It is prudent to carry additional margin prior to testing. Also, spring systems are required, when practical, to have a dynamic force MS over the required force F_a of 25%, as tested. Additionally, when sizing mechanical springs, spring material stress relaxation and residual stresses must be factored in, for which some test data exists [9]. These effects decrease the driving force a spring is capable of after prolonged storage, and can vary by greater than an order of magnitude depending on the material. 302 SS, a common aerospace spring material, can go through 3-5% stress/preload relaxation in 1000 hours of storage time.

The dynamic modeling of springs in this system always considered six compression springs located equidistant around the circumference of the SA interface flange. If incorporated in the final flight design, equivalent redundant pairs of springs will be used to improve reliability. It is important when designing mechanical redundancy to do so wisely as it has been shown that some redundancy can actually decrease overall system reliability, even in spring actuator designs [10], [11].

Pneumatic Actuators: Pneumatic actuators have extensive spaceflight experience, most notably on the Delta launch vehicle stage separation system. Pneumatic actuators possess larger specific force capability (N/kg) than mechanical springs, giving 4 to 5 times the kickoff force of springs of the same mass. Higher part count and pressurized components leads to potentially lower reliability than the simpler mechanical springs, making them less attractive for a crewed mission.

Gas thrusters: While compressed gas thrusters have aerospace flight heritage in solid rocket booster separation (Figure 3) they have no known experience as a spacecraft or payload separation device to this author's knowledge. Their benefit is in producing a large specific force giving very high drive capability, even greater than 10 times that of mechanical springs for the same mass. Where high kickoff forces are not required, their greater complexity and potentially lower reliability may make them less attractive. Gas thrusters are currently being traded against pneumatic actuators for the Ares 1 launch vehicle staging mechanism as well.

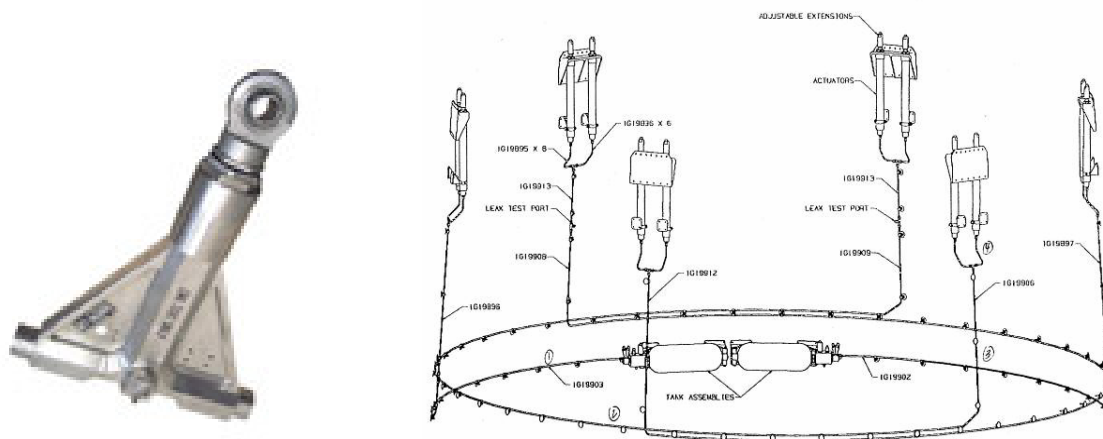


**Figure 3. Pyrotechnic Gas Thruster/Actuator (left), Pneumatic Actuator System (right)
(Used with permission of Scot, Inc.)**

Modeling Approach

To address the mechanism design sizing, two modeling approaches were invoked. Each method allowed for easy evaluations as vehicle configuration changes occurred. The first approach was a simplified Simulink model to quickly assess the critical clearance between the Orion Engine nozzle and the SA. The second approach involved the generation of an Automatic Dynamic Analysis of Mechanical Systems (ADAMS) 3D geometric model to assess secondary effects due to offset mass centers of gravity, off-diagonal moment of inertia terms and other out of plane effects. It also captured any interference due to potential contact between other parts of the Orion Vehicle and the SA.

Simulink Model Approach

The Simulink model approach [12] for the abort simulation was based on the translation and rotational equations of motion which are integrated through the time step function to determine the relative positions of the Ares Upper Stage and Orion. Figure 4 depicts the full Simulink model. The separation force is applied as either a constant pressure (as from a gas thruster) or a variable force (mechanical spring) over the length of the actuation. Assumptions of planar motion for the location of element centers of gravity and constant component masses for the duration of the separation event are incorporated. Capability has been added to the model to include the residual J-2X engine thrust acting on the Ares I US after separation and the contribution of Reaction Control System (RCS) thrust to the separation acceleration.

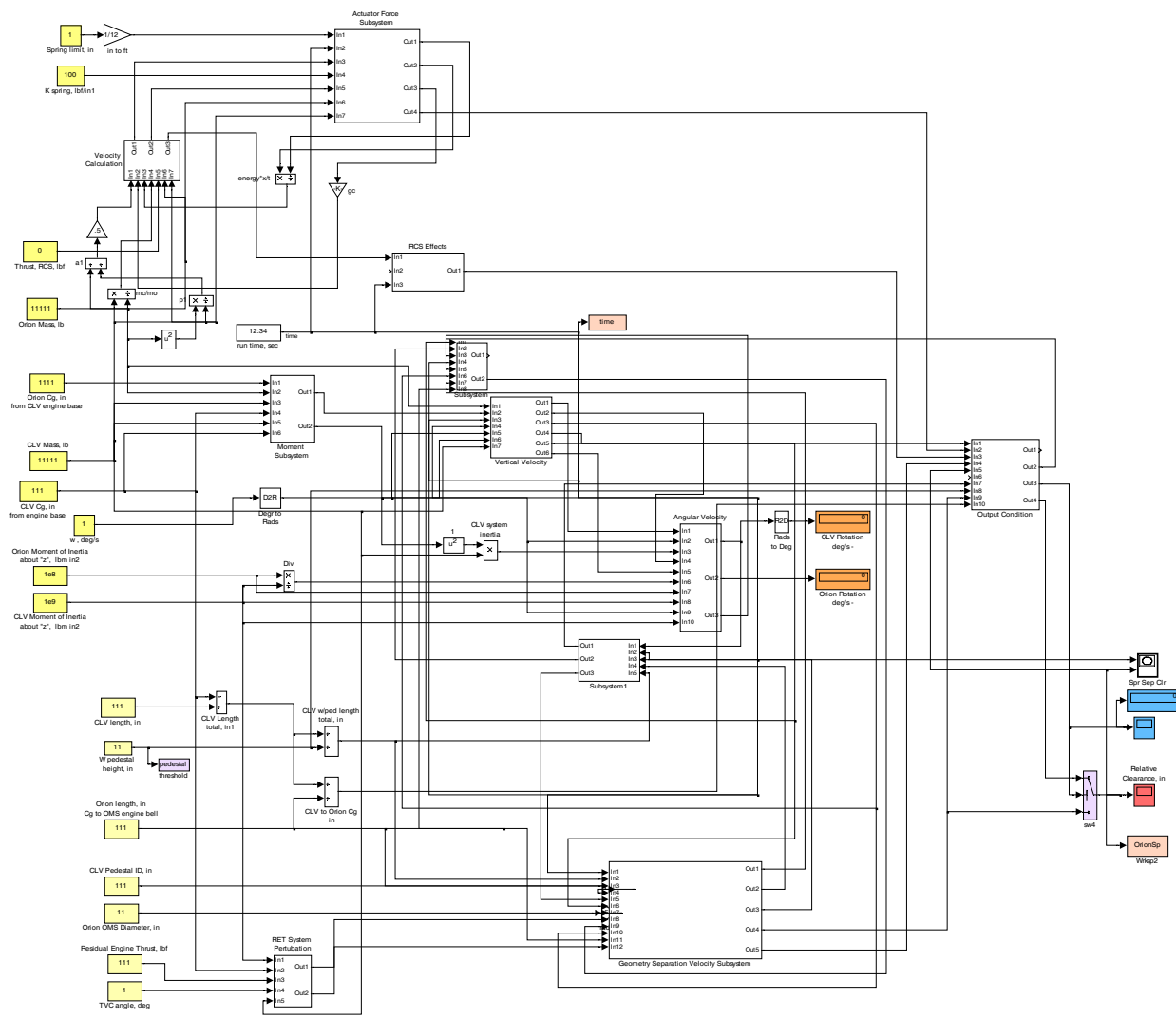


Figure 4. Simulink Separation Model

The basis of the Simulink analysis utilizes the conservation of momentum and kinetic energy equations shown below:

$$(I_{stack} \omega) = (I_C + m_C r_C^2) \omega_C + (I_O + m_O r_O^2) \omega_O$$

and

$$\left(\frac{I_{stack} \omega^2}{2} \right) = \left(\frac{m_C v_C^2 + I_C \omega_C^2}{2} \right) + \left(\frac{m_O v_O^2 + I_O \omega_O^2}{2} \right)$$

Where the variables are defined as:

- I_{stack} = Stack (Orion + Ares 1 US) moment of inertia, kg-m²
- I_C = Ares 1 US moment of inertia, kg-m²
- I_O = Orion moment of inertia, kg-m²

ω	=	body stack rate of rotation, deg/s
ω_c	=	Ares 1 US rate of rotation, deg/s
ω_O	=	Orion rate of rotation, deg/s
m_c	=	Ares 1 US mass, kg
m_O	=	Orion mass, kg
r_c	=	Ares 1 US c_g moment arm to system cg, m
r_O	=	Orion c_g moment arm to system cg, m
v_c	=	Ares 1 US relative velocity to system, m/s
v_O	=	Orion relative velocity to system, m/s

The results of solving these equations are that the rotation rate of the separated components is maintained at the same rate as the stack rotation prior to separation. The addition of a residual engine thrust post separation does induce an additional moment onto the Upper Stage and results in an angular acceleration, reducing the clearance during separation.

ADAMS Approach

The SA/Upper Stage and Orion vehicles were also modeled using the ADAMS dynamic software code [13]. This is a motion simulation code which allows the user to create a mechanism model and then solves the simultaneous equations for kinematic, static, quasi-static, and dynamic simulations. Figure 5 depicts the ADAMS separation model during a simulation as Orion clears the SA. For the purposes of this study the Upper Stage and Orion were modeled as rigid bodies, each with six degrees of freedom (DOF). The SA was modeled as rigidly linked to the Upper Stage since it never separates from it. However the geometry of the SA, particularly the top flange was important for this analysis since the Orion engine nozzle needs to be extracted from this cavity and translate beyond the top flange of the SA without impact. The Crew Module (CM) and SM were modeled as a single rigid body (i.e. Orion) since, again, they never separate in this analysis. The modeling of the separation systems for the Orion to Ares 1 US included the single axis springs or actuators located around the SA top flange, between the SM and SA. These compression springs produce a translational motion when released. Once their free length is achieved they no longer impart any force onto the vehicle. The Ares 1 US's J-2X engine thrust is modeled at the bottom of the Upper Stage. Auxiliary engine thrust is also accounted for on several design studies and these are also modeled as point forces located at the current auxiliary engine locations near the separation plane. Vehicle "dump" or pitch rate is applied as an initial velocity condition to the Ares 1 US/Orion at the combined vehicle stack center of gravity (CG). Joints were added to the model as follows: a fixed joint was created between the Upper Stage and the CEV to allow them to pitch together at the start of the simulation (time = 0 sec.) and release when the separation event began arbitrarily at time = 1.0 sec.; a hinge joint was created at each solar array anchor point under the avionics ring to allow for flaring of the arrays in order to investigate different launch configurations to optimize array clearance from the outer fairings at launch as well as avoid impact with the SA upon separation.

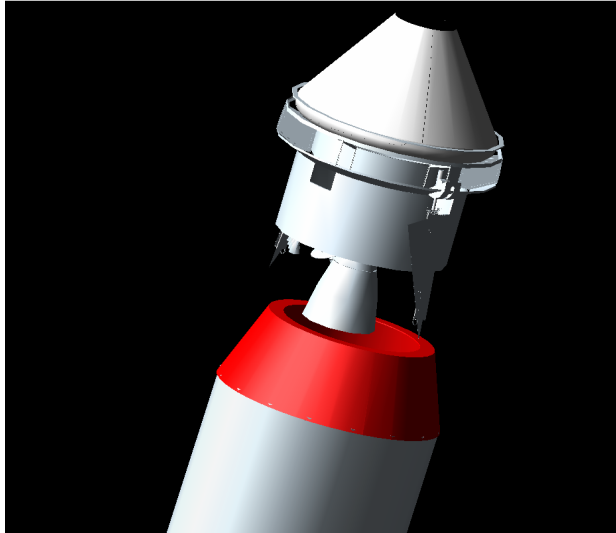


Figure 5. ADAMS Separation Model

Results

The clearance requirement for this system was to provide a 0.051 m (2 in) minimum clearance between the Orion vehicle (engine nozzle, solar arrays, and other protrusions) and the SA. Several analyses were completed to size the actuator forces, determine practical separation times and optimize the vehicle geometry (engine size, solar array placement, SA diameter, etc.). Figure 6 plots the time that the minimum clearance is reached versus the vehicle dump rate for a gas actuator system and for the case of no actuator forces, using the Simulink model. From this plot the two systems are seen to coincide at the higher body rates where the actuation force needed for the 0.051 m (2 in) clearance is diminishing as the system approaches the no-force required condition.

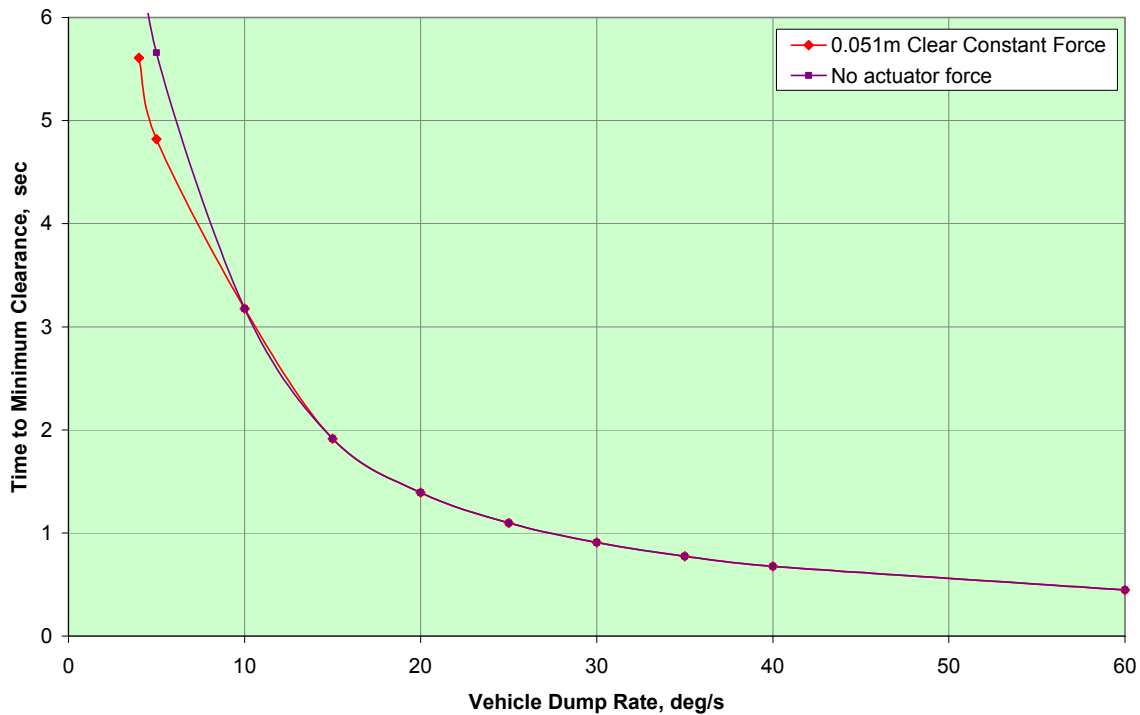


Figure 6. Clearance Time as a Function of Vehicle Body Rate

The initial actuation force required to meet the clearance requirement at the baseline 5 deg/s dump rate is shown in Figure 7. The curves in the figure are the Orion radial clearance (red), the Orion axial separation distance (green), and the actuator force line (blue) which shows when the actuator force is terminated (0.33 sec) and is reflected in the slope of the Orion separation distance curve which tends to be more linear after this force is removed. The jog in the clearance curve occurs when the Orion vehicle clears the SA at approximately 4.8 seconds, which is when the change in clearance becomes a positively sloped line as the vehicles move further apart from each other with no chance of contact.

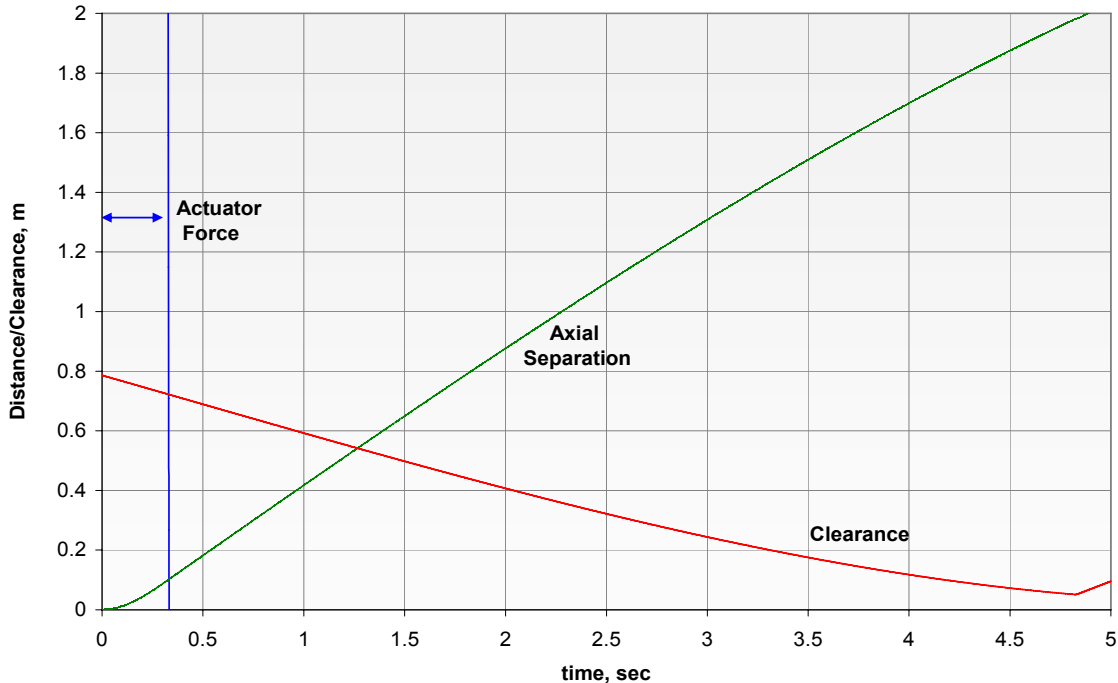


Figure 7. Time Required for Separation at 5 deg/s, (Simulink Model)

Figure 8 is a plot of the Simulink model separation force required to provide clearance at an initial dump rate of 5 deg/s for both types of actuators, springs and gas (or pneumatic) thrusters. In the spring type actuator the force is a function of axial displacement where the initial force is very high and then decreases along a power curve as a function of time. In the gas thruster system, which can be modeled as constant pressure through its full stroke, the force is maintained throughout the action time at a constant level. Both systems were sized to separate the vehicle with exactly 0.051m (2 in) clearance maintained at the engine nozzle. Duration of the constant pressure actuator is determined by the 0.102 m (4 in) actuator stroke. The calculated time necessary to provide this clearance is shown to be independent of the actuation method, since the vehicles are rotating and translating at a rate as a function of dump rate and the residual engine thrust on the Upper Stage. The 0.051 m (2 in) minimum clearance point in space or “gate” is reached at the same point in time, which varies from 24.0 deg (4.8 s) to 23.4 deg (0.39 s) of vehicle rotation for the 5 deg/s to 60 deg/s body rate respectively.

There is a very slight difference in the final velocity induced by the actuators since to make the clearance gate time, the spring actuator provides a higher initial acceleration and then coasts at the resulting velocity of 0.477 m/s (1.56 ft/s) with an acceleration rate of 0.144 g’s, while the constant pressure actuator provides an acceleration rate of approximately 0.118 g’s over a longer time period resulting in a higher 0.485 m/s (1.59 ft/s) final velocity imparted on the Orion system. Therefore, less energy is required for the spring actuator compared to the gas thruster mechanism.

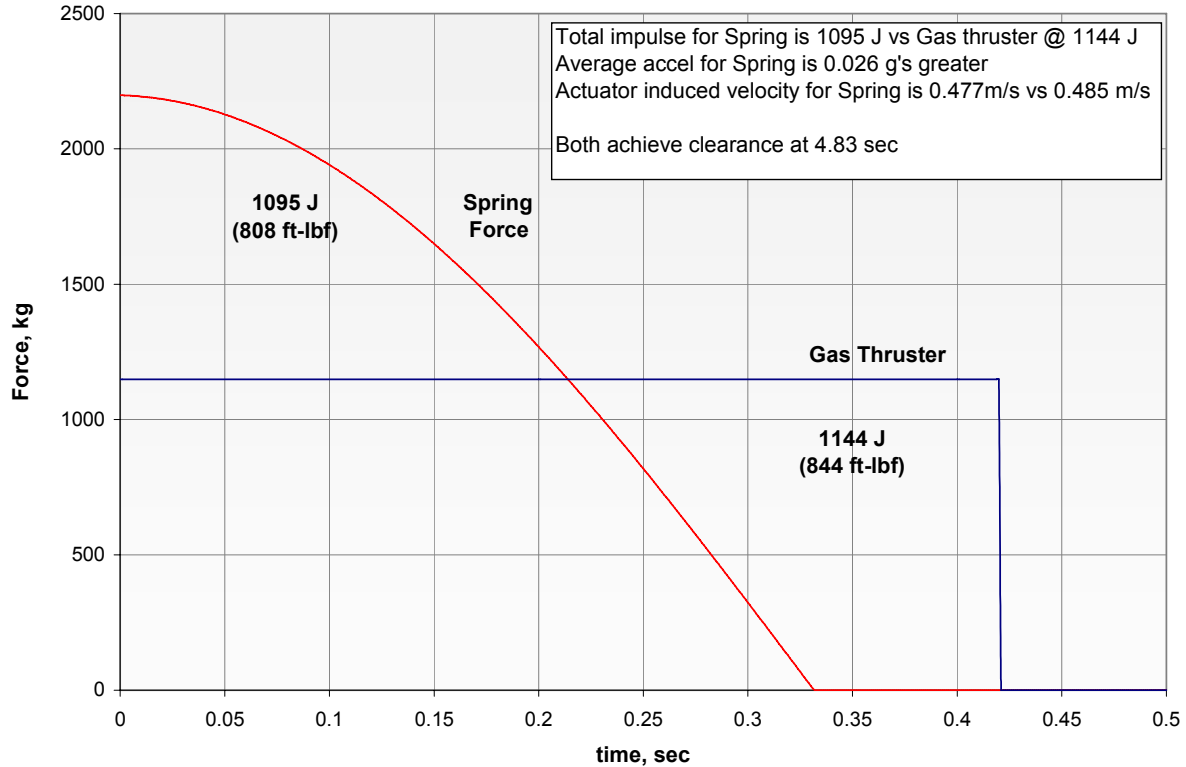


Figure 8. Separation Force Input for Spring vs. Gas Thruster

For the ADAMS model several cases and design studies have been run to determine the optimal separation system. The two critical considerations in these dynamics analyses are to ensure that the SM engine bell can get extracted from within the SA without bumping (avoiding a Falcon 1 type of hazard), and that the solar arrays, which are mounted down the sides can clear the SA without interfering from the outside. Using the given mass properties the resulting spring stiffness case results are shown in Table 1 as well as Figure 9. All cases are assuming there is no separation assistance from the Orion SM main engine.

Table 1. Summary of Parameters Analyzed

case #	dump rate (deg/s)	J-2X Residual Thrust	CEV RCS Thrust kg (lbf)	Spacecraft Adapter flange ID m (in)	Spring stiffness kg/m (lb/in)	Spring stroke length m (in)	min clearance, ADAMS model m (in)	min clearance, Simulink model m (in)	model delta m (in)
1	35	yes	0	3.4 (135)	0	0.102 (4)	0.14 (5.6)	0.11 (4.5)	0.03 (1.1)
2	0	yes	0	3.4 (135)	10,724 (600)	0.102 (4)	0.80 (31.5)	0.72 (28.3)	0.08 (3.3)
3	10	yes	0	3.4 (135)	178 (10)	0.102 (4)	0.07 (2.6)	0.08 (3.0)	-0.01 (-0.4)
4	10	no	0	3.4 (135)	178 (10)	0.102 (4)	0.15 (6.0)	0.13 (5.2)	0.02 (0.8)
5	20	no	0	3.4 (135)	178 (10)	0.102 (4)	0.15 (5.9)	0.13 (5.1)	0.02 (0.8)
6	20	yes	0	3.4 (135)	178 (10)	0.102 (4)	0.13 (5.2)	0.10 (4.1)	0.03 (1.1)
7	5	yes	0	3.15 (124)	4,147 (232)	0.102 (4)	-0.08 (-3.3)	-0.05 (-1.9)	-0.04 (-1.4)
8	35	no	0	3.15 (124)	0	0.102 (4)	0.01 (0.2)	0.01 (0.2)	0
9	5	yes	366 (808)	3.4 (135)	0	0.102 (4)	0.18 (7.2)	0.11 (4.5)	0.07 (2.7)
10	5	yes	0	3.4 (135)	4,147 (232)	0.102 (4)	0.05 (2.0)	0.08 (3.2)	-0.03 (-1.2)

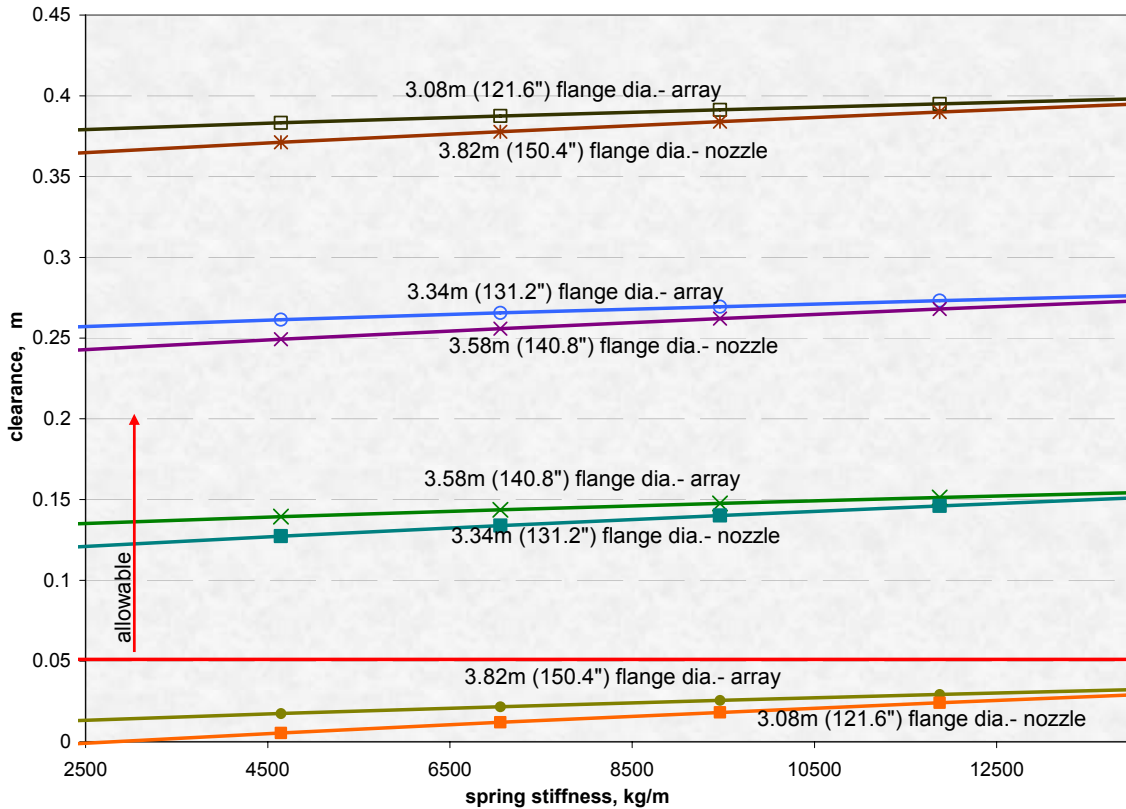


Figure 9. Engine bell and 6m Array clearance for 5°/sec dump rate

Figure 9 depicts the results of several ADAMS cases using different SA flange diameters to assess clearing the solar arrays on the outside versus clearing the engine nozzle on the inside. Previous Orion designs incorporated a longer but narrower vehicle with a likewise narrower SA. The redesign of the vehicle allowed for a wider SA flange. As can be seen in the plot, the arrays have adequate clearance (>0.051m) for any SA inner diameter of 3.58 m (140.8 in) or less, while the engine nozzle will have adequate clearance for a SA diameter of 3.34 m (131.2 in) or greater. Thus an inside diameter of 3.34 – 3.58 m (131.2 – 140.8 in) satisfies both. In these cases it is assumed that the J-2X engine residual thrust is active and the flange width is 0.343 m (13.5 in) radially. A nominal separation system would include springs located at SA nodes as shown in Figure 2 outboard of the separation pyrotechnic device with a 0.102 m (4 in) stroke and 3,842 kg/m (215 lb/in) stiffness. Six standard 0.0127 m (1/2 in) separation bolts located directly inboard of the push off springs at each node will transmit launch loads through the structure.

Figure 10 is a plot of the separation clearance as a function of time for the different models used for the baselined configuration at a body rate of 5 deg/s. The ADAMS model includes the Solar Arrays for additional clearance studies while the Simulink model only considers the clearance for the Engine Nozzle to the SA, which becomes the limiting parameter for both models after approximately 2.4 seconds.

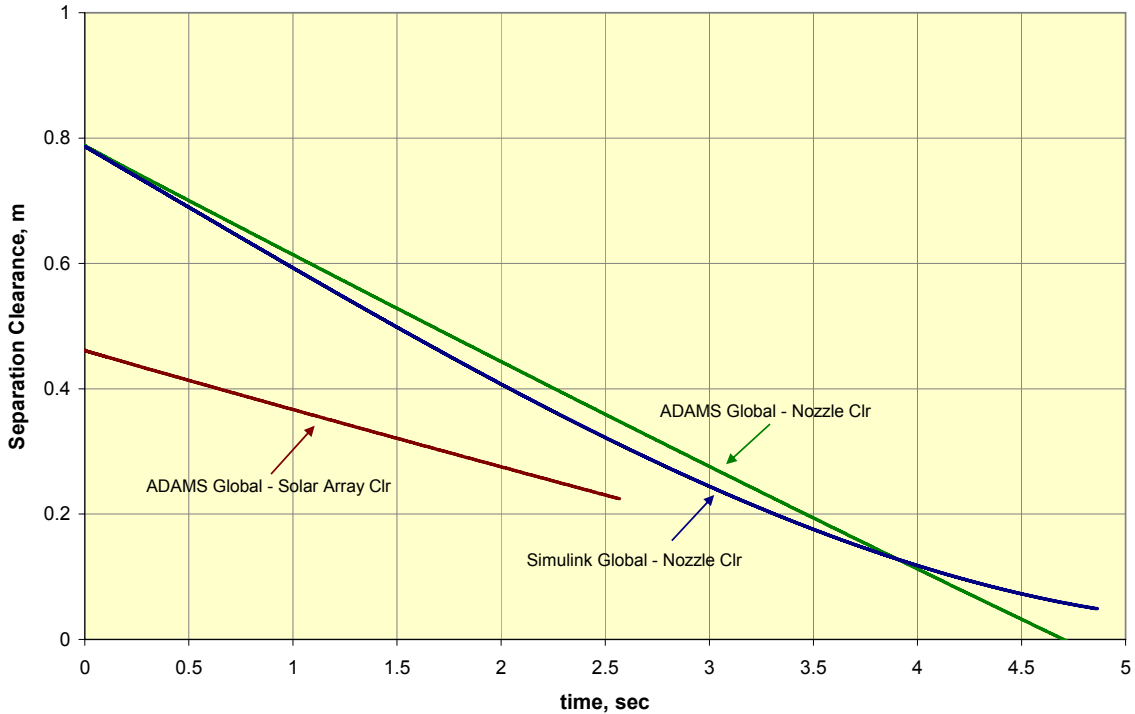


Figure 10. Separation Clearance at 5 deg/s Body Rate

Figure 11 depicts the clearance achieved as a function of actuator force for the Simulink and ADAMS models at a 5 deg/s dump rate. The interference at the low actuator force is due to the influence of the applied RET moment and to the longer separation time required for the low dump rates (<10 deg/s). This slower separation time allows the induced moment on the Upper Stage to rotate the SA reducing the clearance below the required limit. From the plot it is evident that an actuator force of greater than 3500 kg/m (196 lb_f/in) is required to assure the clearance is achieved and that use of a grossly oversized actuator has diminishing returns since the actual clearance is not a linear function of spring stiffness.

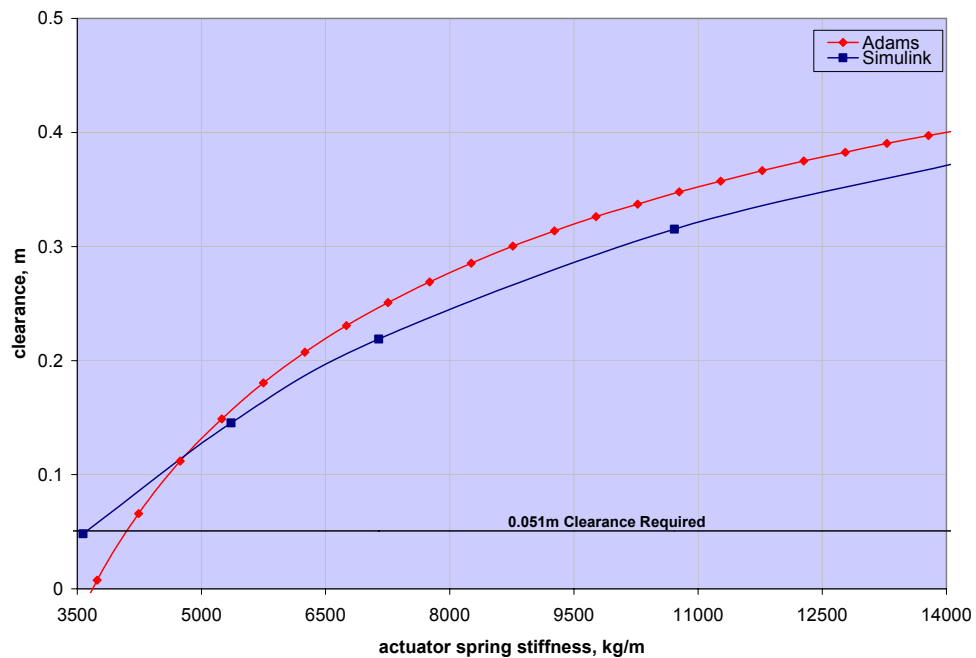


Figure 11. Comparison of Clearance vs. Actuator Force

Natural Separation

It has been learned through this analysis that for two bodies rigidly fixed together and undergoing rigid body rotational and translational motion which then separate, if body 1 has a protruding feature (like an engine bell) tucked inside a recessed area of body 2 (such as the SA cavity) that, due to the centrifugal forces naturally propelling them apart, there exists a relationship between the diameter and length of the protruding feature and the mating clearing radius Y_{B1} of the recess whereby for a recess radius greater than Y_{B1} , the vehicles will separate without collision at any dump rate with no additional kickoff force required nominally. Figure 12 depicts the geometry definitions used.

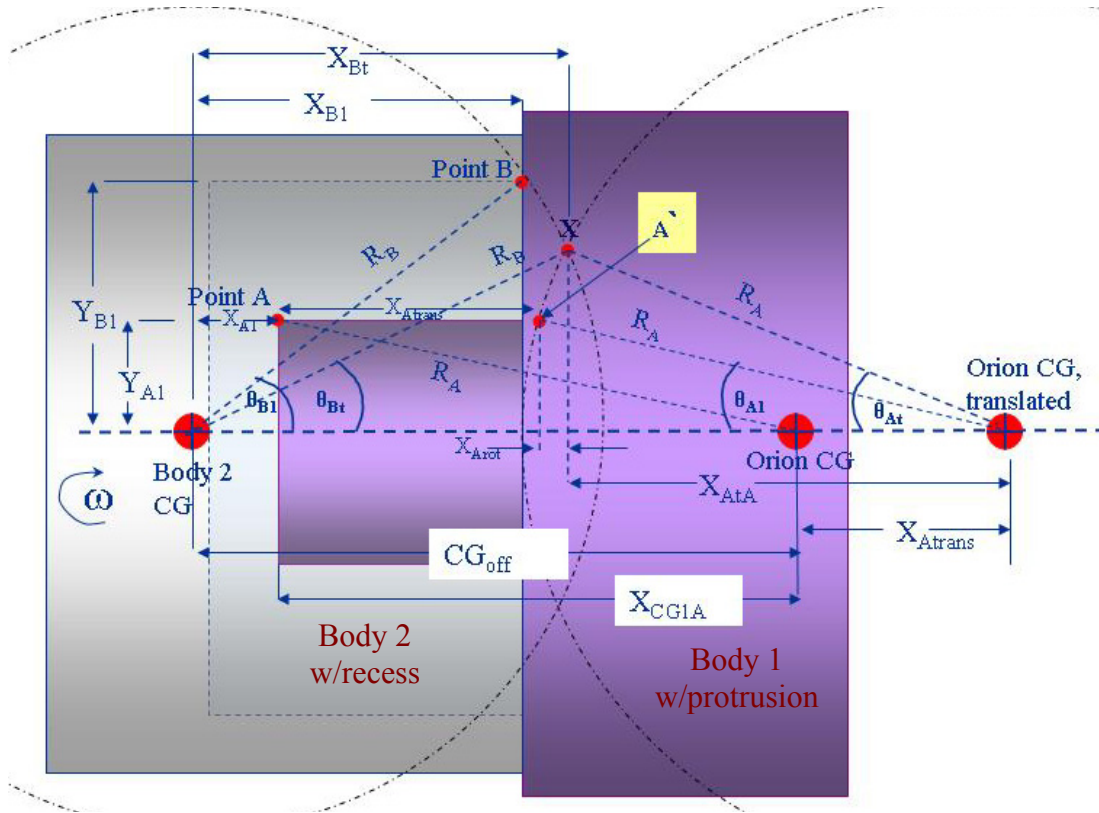


Figure 12. Ares I US/Orion Vehicle Geometry and Definition

$R_B \cdot \cos(\theta_{Bt}) = X_{A1} + X_{Atrans} + X_{Arot}$; where X_{A1} is the initial axial distance from Body 2 CG to Protrusion point A, X_{Atrans} and X_{Arot} depict the axial & rotation motion components of point A, which represents the outermost point of the protrusion.

$$R_B = R_A \cdot (\sin(\theta_{At}) / \sin(\theta_{Bt}))$$

$$\sin(\theta_{A1}) = Y_{A1} / R_A$$

$$R_B = \sqrt{(X_{B1})^2 + (Y_{B1})^2}$$

$$X_{CG1A} + X_{A1} = CG_{off}; \quad CG_{off} \text{ is the distance between Body 1 and 2 CG's prior to separation.}$$

$$X_{Atrans} = \omega \cdot T_{coll} \cdot CG_{off}; \quad T_{coll} \text{ is the time needed for pt. A to separate and pass thru pt. B at X.}$$

$$X_{Arot} = R_a \cdot [\cos(\theta_{A1}) - \cos(\theta_{At})]$$

$$X_{Bt} = R_B \cdot \cos(\theta_{Bt})$$

$$X_{Bt} + X_{AtA} = CG_{off} + X_{Atrans}$$

$$\theta_{Bt} = \theta_{B1} - \omega \cdot T_{coll}$$

$$\theta_{At} = \theta_{A1} + \omega \cdot T_{coll}$$

Thus, the minimal recess radius for natural separation, Y_{B1} , can be solved for easily, if X_{A1} , Y_{A1} (protrusion radius), and lengths X_{B1} (recess radius) and CG_{off} (distance between CG's) are known. This analysis

assumes the protrusion and recess are modeled as straight cylinder sections. This finding gives a designer a useful preliminary size for the vehicle recess diameter (such as in a spacecraft adaptor cone flange) or protruding diameter (such as an engine bell), and is independent of the vehicle's dump rate at separation. While this does not account for secondary effects like residual engine thrusts and separation event side loads, tank slosh or friction which can either help or hurt this clearance, these effects are typically secondary to the overall conic area that the bodies follow dynamically upon separation. For our case, assuming no external forces, the separation event has been determined to occur naturally for the approximately 28.5 degrees of rotation needed and will provide a minimum clearance of 0.173 m (6.8 in) for all significant body rates. This is primarily due to the location of the Vehicle Stack system Cg which is located very close to the separation plane and is therefore very sensitive to any changes in that location.

Taking this concept further, separation cases were run (see figure 13) in which the same conditions were applied to a vehicle with an adequately large recess diameter (SA flange diameter) and to an undersized flange diameter (124 in). As can be seen, cases were run with the US engine on or off for comparison. As the lowest curve shows for a smaller SA flange of 3.15 m (124 in), spring force is dependent on dump rate as the higher dump rates require much larger spring stiffness to clear upon separation, while for a SA flange ID of 3.4 m (top curve) no springs are required at any dump rate even with the US engine on (2nd curve). The vehicle separates naturally without help of any kickoff device.

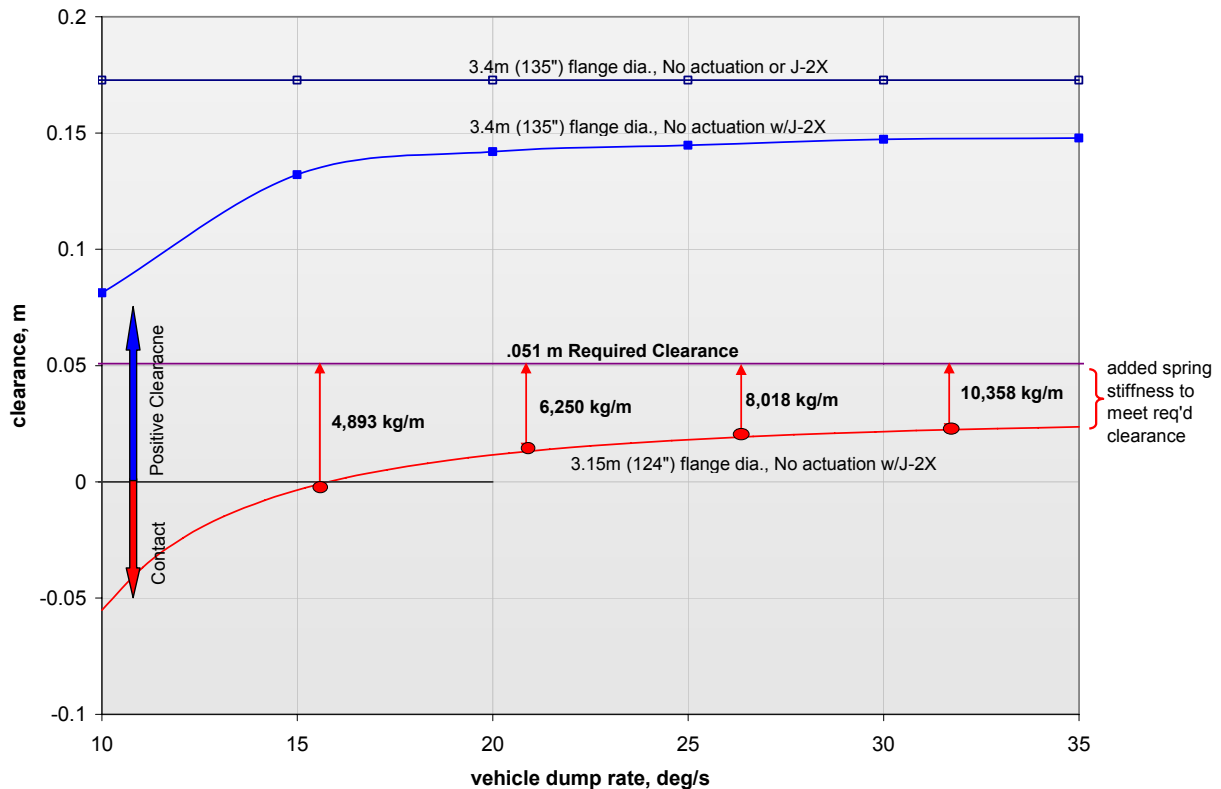


Figure 13. Engine Nozzle Clearance with No Separation Forces (no springs or actuators)

Lessons Learned

One of the lessons learned was that intelligent preliminary sizing of spacecraft geometry can greatly improve reliability and save on vehicle weight. Also for two connected bodies rotating at a fixed dump rate, that same angular rate will be maintained by each body after separation, as angular momentum is conserved. Another important lesson learned was that separation mechanism component mass can be

minimized and reliability maximized if the geometry is dimensioned to allow for “natural separation” concepts. However, the need for a controlled separation event necessitates the use of applied force actuators to overcome any potential external forces. The last lesson learned was that there exists a very steep curve between separation clearance and the vehicle main parameters of mass, inertia and geometry with that sensitivity often resulting in inadequate clearance dynamics.

Summary

The simulations conducted indicate that a low fidelity, 2-D equations of motion model can be useful in separation mechanism design. It provides insight into separation events and the many parameters and their relative sensitivities. A more detailed 3-D geometric dynamics model is also required to clearly define the actuator requirements while accounting for all factors in three dimensions and can also identify interferences due to other hardware on the vehicle. The overall design conclusions drawn are that a simple, dependable spring system can be used for the Orion crewed vehicle separation system. Minimizing the actuator force is preferred in terms of mass, reliability, and cost. However, ensuring the separation system controls the event and all potential external forces is still paramount. This is especially true in an abort scenario. Additional effort needs to be invested to assure second order effects due to propellant slosh or thruster imbalance does not violate the design criteria used in the analysis.

Acknowledgments

The authors would like to acknowledge the contributions, advice, and suggestions of Keith Schlagel and Lance Lininger of Lockheed Martin Corporation which aided in the development and compilation of this work.

References

1. <http://www.spacex.com/media.php?page=57>
2. Onoda, J. “The Development of Staging Mechanisms for the Japanese Launcher Mu-3SII,” 19th Aerospace Mechanisms Symposium, NASA Ames Research Center, August, 1985.
3. Harrington, T.G. “Compression Spring Separation Mechanisms,” First Aerospace Mechanisms Symposium, University of Santa Clara, Santa Clara, California, May 19-20, 1966.
4. Abdul Majeed, M. K., Matarajan, K., Krishnankutty, V. K. “Separation and Staging Mechanisms for the Indian SLV-3 Launch Vehicle,” 18th Aerospace Mechanisms Symposium, NASA Goddard Space Flight Center, May 1984.
5. AIAA-S-114-2005, *Moving Mechanical Assemblies Standard for Space and Launch Vehicles*, American Institute of Aeronautics and Astronautics standard, July 2005.
6. Conley, Peter L. *Space Vehicle Mechanisms*, New York, John Wiley & Sons, Inc. 1998.
7. Brennan, Paul C., *NASA Space Mechanisms Handbook*, July 1999.
8. Purdy, W., Hurley, H., “The Clementine Mechanisms,” 29th Aerospace Mechanisms Symposium, NASA Johnson Space Center, May 1995.
9. Hanna, W. D., Chang, R. S., Sheckel, G. L., “Stress Relaxation of Spring Materials,” Fortieth Anniversary: Pioneering the Future, May 1998.
10. Chew, M. “On the Danger of Redundancies in Some Aerospace Mechanisms,” 22nd Aerospace Mechanisms Symposium, NASA Langley Research Center, May 1988.
11. Holmanns, W., Gibbons, D., “Misconceptions in Mechanical Reliability,” 34th Aerospace Mechanisms Symposium, NASA Goddard Spaceflight Center, May 2000.
12. Simulink program Ver.7.0.1.29704, The Math Works Corporation, September 2004.
13. ADAMS dynamic software code Ver. 2005 r2.0, MSC Software Corporation, August 2005.